MucosalImmunology

www.nature.com/mi

ARTICLE

A gammaherpesvirus licenses CD8 T cells to protect the host from pneumovirus-induced immunopathologies

Mickaël Dourcy[1], Céline Maquet[1], Lorène Dams[1], Gautier Gilliaux[2], Justine Javaux[1], Daniel Desmecht[2], Matthias Mack[3], Benjamin G. Dewals[1], Bénédicte Machiels[1] and Laurent Gillet[1]

Human respiratory syncytial virus (RSV) is a pneumovirus that causes severe infections in infants worldwide. Despite intensive research, safe and effective vaccines against RSV have remained elusive. The main reason is that RSV infection of children previously immunized with formalin-inactivated-RSV vaccines has been associated with exacerbated pathology, a phenomenon called RSV vaccine-enhanced respiratory disease. In parallel, despite the high RSV prevalence, only a minor proportion of children develop severe diseases. Interestingly, variation in the immune responses against RSV or following RSV vaccination could be linked with differences of exposure to microbes during childhood. Gammaherpesviruses (γHVs), such as the Epstein–Barr virus, are persistent viruses that deeply influence the immune system of their host and could therefore affect the development of pneumovirus-induced immunopathologies for the long term. Here, we showed that a previous γHV infection protects against both pneumovirus vaccine-enhanced disease and pneumovirus primary infection and that CD8 T cells are essential for this protection. These observations shed a new light on the understanding of pneumovirus-induced diseases and open new perspectives for the development of vaccine strategies.

Mucosal Immunology (2020) 13:799–813; https://doi.org/10.1038/s41385-020-0293-7

INTRODUCTION

Human respiratory syncytial virus (RSV) is a major cause of severe lower respiratory tract infection in infants worldwide and is also recognized as an important pathogen in adults, especially the elderly.[1] Despite intense research efforts, safe and effective vaccines have remained elusive.[2] One chief explanation resides in the history of RSV vaccine-enhanced respiratory disease.[3] Indeed, RSV infection of some children previously immunized with a formalin-inactivated (FI)-RSV vaccine has been associated with exacerbated disease and pulmonary eosinophilia as a result of a putative dysregulated memory Th2 response.[4] In parallel, there is a wide variation in the immune responses against RSV primary infection. Thus, while the majority of children have been infected with RSV at least once by 2 years of age, only some infected infants develop severe lower respiratory tract infection.[5] It appears that the predisposition of some children to these two RSV-induced immunopathologies could be related to extrinsic factors affecting the development of the immune system in early life.[6] Thus, several studies have highlighted that microbiome composition can impact the development of RSV pathogenesis.[6] Microbes play fundamental roles in controlling many aspects of host physiology and in particular immune responses. Until recently, researches focussed mainly on the influence of microbiota. However, immune imprinting by viruses is also a key determinant for variation in disease susceptibility.[7–9] In particular, persistent viruses such as gammaherpesviruses (γHVs) have coevolved with their host and appear to broadly influence the composition and function of the immune system.[10,11] The human γHV Epstein–Barr virus (EBV) infects more than 90% of people worldwide. Interestingly, while EBV infection occurs usually during childhood, recent epidemiological surveys highlighted an increased age of seroconversion to EBV in developed countries.[12] We therefore hypothesized that the sequence following which children encounter γHVs and RSV in the early age might influence the outcome of RSV infections.

EBV is host specific, and the study of RSV has been hampered by its poor replication in animal models.[13] The use of Murid Herpesvirus 4 (MuHV-4) and of the pneumonia virus of mice (PVM) provides therefore some robust mouse models for studying these infections in a natural host–pathogen relationship.[14,15] PVM may also serve as a useful model to investigate the mechanisms underlying the Th2-skewed hypersensitivity observed after vaccination with formalin-inactivated (FI) antigens (Ags).[16] Moreover, MuHV-4 infection has been shown to train immunity against various heterologous infections.[17–19] Besides, in line with the hygiene hypothesis,[20–22] we have recently observed that respiratory infection with MuHV-4 confers long-lasting protection against airway allergy through the replacement of resident alveolar macrophages (AMs) with recruited regulatory monocytes of bone marrow origin.[11] In the present study, we have investigated whether a previous γHV infection could induce bystander beneficial modulations shaping the immune responses to pneumovirus infection.

RESULTS

MuHV-4 infection confers protection against PVM vaccine-enhanced disease

To investigate whether a γHV infection could modulate subsequent pneumovirus vaccine-related Th2 immunopathology, we

[1]Immunology-Vaccinology Laboratory, Department of Infectious and Parasitic Diseases, FARAH, University of Liège, 4000 Liège, Belgium; [2]Pathology, Department of Morphology-Pathology, FARAH, University of Liège, 4000 Liège, Belgium and [3]Regensburg University Medical Center, Regensburg, Germany
Correspondence: Bénédicte Machiels (bmachiels@uliege.be) or Laurent Gillet (L.gillet@uliege.be)
These authors contributed equally: Bénédicte Machiels, Laurent Gillet

Received: 17 September 2019 Revised: 25 March 2020 Accepted: 31 March 2020
Published online: 18 May 2020

infected BALB/c mice with MuHV-4 (Fig. 1a) and 30 days post infection (p.i.), a period allowing latency establishment (Supplementary Fig. 1),[23] mice received either FI-PVM Ags vaccine or Control Ags (Ctrl Ags) before being challenged a week later i.n. with live PVM or PBS as control. Mice were euthanized 5 days after challenge and respiratory immune responses were compared between groups. Typical features of pneumovirus vaccine-induced immunopathology were observed in Mock-infected mice subjected to FI-PVM vaccination and subsequent PVM challenge (Mock/FI-PVM/PVM). We observed infiltration of eosinophils in

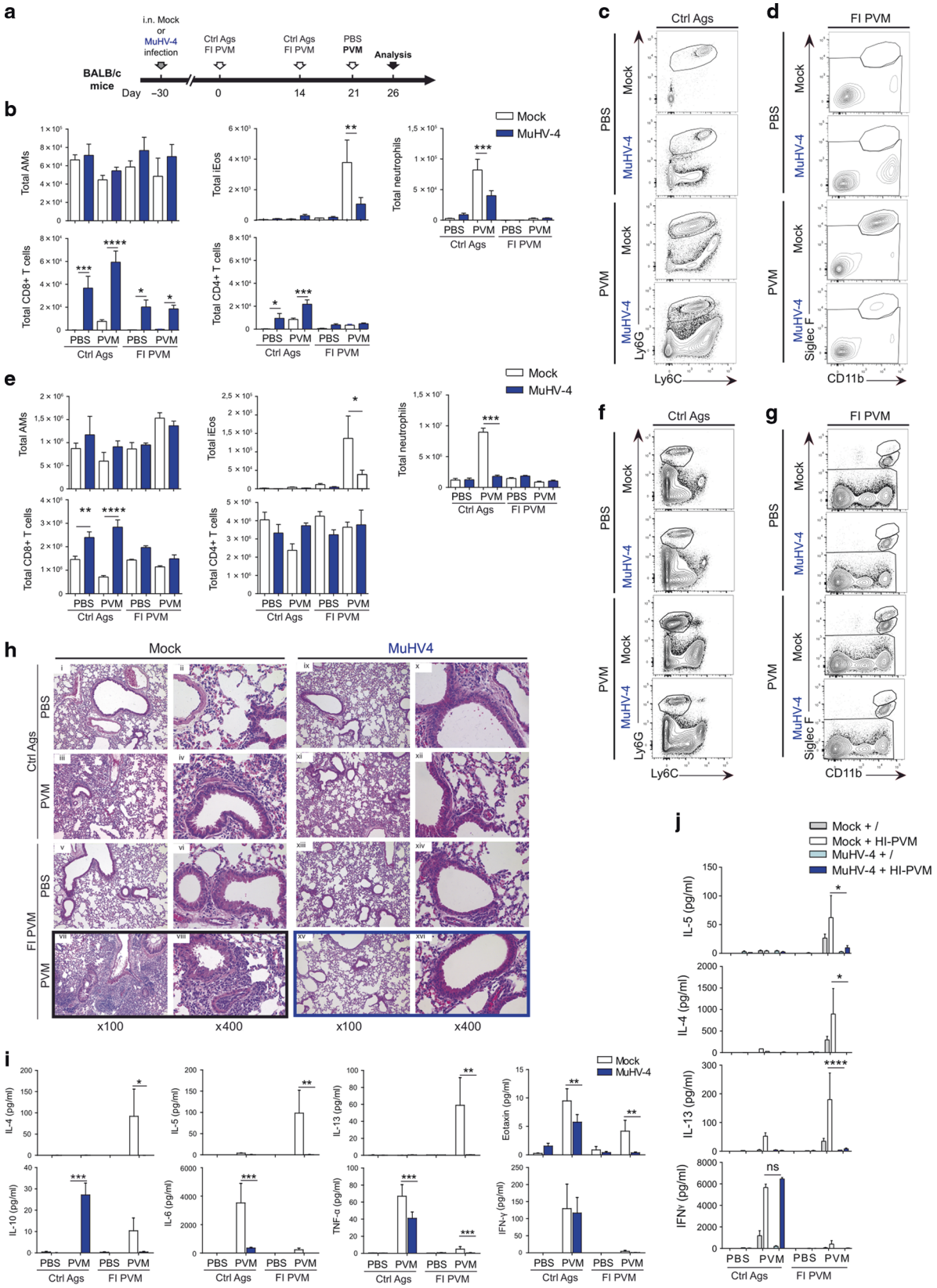

Fig. 1 MuHV-4 infection inhibits the development of PVM-induced immunopathologies. a–j Thirty days after i.n. Mock or MuHV-4 infection, BALB/c mice were vaccinated (2 s.c. injections of 10 µg of FI-PVM Ags or Ctrl Ags in 100 µL PBS at 14 days intervals), then challenged i.n. with 3.10^2 PFU of PVM (or PBS) and euthanized 5 days later. Experimental outline (**a**). Absolute numbers of total leucocytes, AMs, lymphocytes, eosinophils and neutrophils in BALF (**b**) and in lung (**e**). Flow cytometry of BALF eosinophils (gated as live non-autofluorescent $SSC^{hi}CD11b^{int}SiglecF^{+}$) (**c**) and neutrophils (gated as live non-autofluorescent $CD11c^{-}SSC^{int}CD11b^{+}Ly6G^{+}$) (**d**). Flow cytometry of lung inflammatory eosinophils (gated as live $CD45^{+}$ non-autofluorescent $SSC^{hi}CD11c^{-}CD11b^{+}SiglecF^{hi}$) (**f**) and neutrophils (gated as live $CD45^{+}$ non-autofluorescent $SSC^{int}CD11c^{-}SiglecF^{-}CD11b^{+}Ly6G^{+}$) (**g**). Histological analysis of lung sections stained with hematoxylin and eosin (H&E) (**h**). Cytokines concentration in BALF (**i**) and in supernatants of MLN cells assessed with or without restimulation for 3 days ex vivo with heat-inactivated PVM (HI-PVM) (**j**). Data are presented as means ± SEM. $*P \le 0.05$; $**P \le 0.01$ and $***P \le 0.001$ (one-way ANOVA and Bonferroni post-tests). Data are representative of at least three independent experiments with five mice per group.

lung parenchyma (Fig. 1b–d) as well as in the airways (Fig. 1e–g). Interestingly, in lung parenchyma, we were able to distinguish that these infiltrating eosinophils were inflammatory eosinophils, characterized by a high expression of SiglecF.[24] In contrast, MuHV-4-infected mice exposed to the same treatments (MuHV-4/FI-PVM/PVM) displayed a reduced recruitment of inflammatory eosinophils, and an increased infiltration of CD8 T cells in the airways. These results were confirmed by histological analysis that revealed peribronchial and perivascular infiltrates of mononuclear cells, eosinophils (Fig. 1h). Analysis of cytokines in bronchoalveolar lavage fluids (BALF) revealed increased levels of interleukin (IL)-4, IL-5, IL-13 and eotaxin in Mock/FI-PVM/PVM mice (Fig. 1i). In contrast, there was less production of these cytokines in MuHV-4/FI-PVM/PVM mice, arguing for a reduced Th2 response (Fig. 1i). Finally, mediastinal lymph node (MLN) cells from MuHV-4 FI-PVM/PVM produced less IL-4, IL-5 and IL-13 after in vitro restimulation with heat-inactivated-PVM Ags than MLN cells from Mock/FI-PVM/PVM mice while IFNγ productions were similar (Fig. 1j). The protection conferred by MuHV-4 relied on primary live infection as i.n. administration of the same amount of inactivated MuHV-4 does not have any effect (data not shown).

The difference in Th2 immune response could be consecutive to differences in PVM Ag loads at challenge, therefore, to equalize the amount of PVM Ags, FI-PVM vaccinated mice were challenged with inactivated PVM (Supplementary Fig. 2a). This experiment confirmed the strong inhibition of the PVM-induced Th2 immunopathology in MuHV-4-infected mice as indicated by the quasi-absence of eosinophils and neutrophils in BALF (Supplementary Fig. 2b) and the reduced lung inflammation (Supplementary Fig. 2b, c). To assess a potential plasticity of the Th2 CD4 T cells towards a regulatory phenotype following MuHV-4 infection,[25,26] we examined the proportions of FoxP3 and GATA-3-expressing CD4 T cells in MLN. While we did not see any difference in percentages of FoxP3+ cells or any FoxP3 + GATA-3 + double positive cells (not shown), we observed a significant reduction of GATA-3 expressing cells in MuHV-4/FI-PVM/PVM mice compared with Mock/FI-PVM/PVM mice (Supplementary Fig. 2d, e).

Finally, as the decreased inflammation in MuHV-4-infected mice could arise from a delayed PVM replication, groups of mice treated as in Fig. 1 were successively euthanized at days 5, 6 and 7 after i.n. PVM challenge (Supplementary Fig. 3a). The most severe inflammatory response occurred at day 6 post-PVM challenge in Mock/FI-PVM/PVM mice. In contrast, we observed a massive reduction in the number of BALF eosinophils in MuHV-4/FI-PVM/PVM mice regardless of the day post-PVM challenge (Supplementary Fig. 3b).

MuHV-4 infection confers clinical protection against heterologous PVM primary infection

Besides the inhibition of PVM-induced Th2 response, lung MuHV-4 infection also seems to have major consequences in the context of PVM primary infection. Indeed, inflammation was significantly reduced in MuHV-4/Ctrl Ag/PVM compared with Mock/Ctrl Ag/PVM mice (Fig. 1 and Supplementary Fig. 3) as revealed by the strong reduction of the number of BALF and lung neutrophils in MuHV-4/Ctrl Ags /PVM mice in comparison with Mock/Ctrl Ags/PVM mice (Fig. 1b, c, e, f and Supplementary Fig. 3). Moreover, high levels of IL-6 and TNF-α were observed in Mock/Ctrl Ags/PVM mice as described,[27,28] while these levels were strongly reduced in MuHV-4/Ctrl Ags/PVM mice (Fig. 1i). In contrast, IFN-γ release was not affected in BALF from MuHV-4-infected mice (Fig. 1i), indicating that MuHV-4 infection does not impair the production of all cytokines.

In its natural host, the highly pathogenic strain PVM J3666 is characterized by robust viral replication in lungs leading to marked morbidity, weight loss, and mortality in response to a minimal viral inoculum. Accordingly, we observed that, in absence of MuHV-4 infection, mice displayed a severe weight loss starting at day 5 after PVM inoculation (Fig. 2b) that required euthanasia upon exceeding the weight loss threshold (25%). In contrast, while MuHV-4 primary infection was associated with a moderate and transient weight loss (from day 6 to day 12), these MuHV-4-infected mice did not show any weight loss nor clinical signs upon PVM challenge and survived the infection (Fig. 2b, c).

MuHV-4 infection induces a significant reduction of PVM loads in lungs

We next quantified PVM viral loads in lungs of the different groups (Fig. 3). First, infectious PVM virions in lungs were quantified by plaque assay during 3 consecutive days after PVM challenge (Fig. 3b). While FI-PVM vaccinated mice displayed lower PVM titres, high PVM titres were detected in non-vaccinated groups. Interestingly, MuHV-4/Ctrl Ags/PVM mice showed significantly reduced PVM titres (Fig. 3b). These results were confirmed by quantification of PVM genomic copies at day 6 after PVM infection (Fig. 3c). To see if the protection conferred by MuHV-4 against PVM replication could be explained by the improvement of early antibody response, we characterized the anti-PVM neutralizing antibody titres in the different groups (Fig. 3d). Results showed development of neutralizing antibodies following FI-PVM vaccination without any significant difference between Mock and MuHV-4-infected mice. Noticeably, in absence of previous FI-PVM vaccination, PVM infection did not induce protective levels of neutralizing antibodies at day 6 p.i. neither in Mock nor in MuHV-4-infected mice. Thus, collectively, these findings showed that MuHV-4 infection does not modulate the development of humoral adaptive response but improves the early control of PVM replication.

MuHV-4 infection modulates the pulmonary response against PVM challenge

To distinguish between local and systemic effects of MuHV-4 infection on the Th2 response, we firstly submitted FI-PVM vaccinated Mock or MuHV-4-infected mice to respiratory or footpad PVM challenges and assessed levels of proliferation and cytokine production by MLN and popliteal lymph nodes (PLN) cells respectively (Fig. 4). While this Ag recall assay confirmed a lower production of IL4, IL5 and IL13 by MLN cells from MuHV-4/FI-PVM/PVM mice compared with those from Mock/FI-PVM/PVM, the proliferation and production of Th2 cytokines by PLN cells were similar between groups (Fig. 4c). Interestingly, level of IFNγ was comparable between Mock or MuHV-4 infected groups regardless of the challenge site. This suggests that MuHV-4

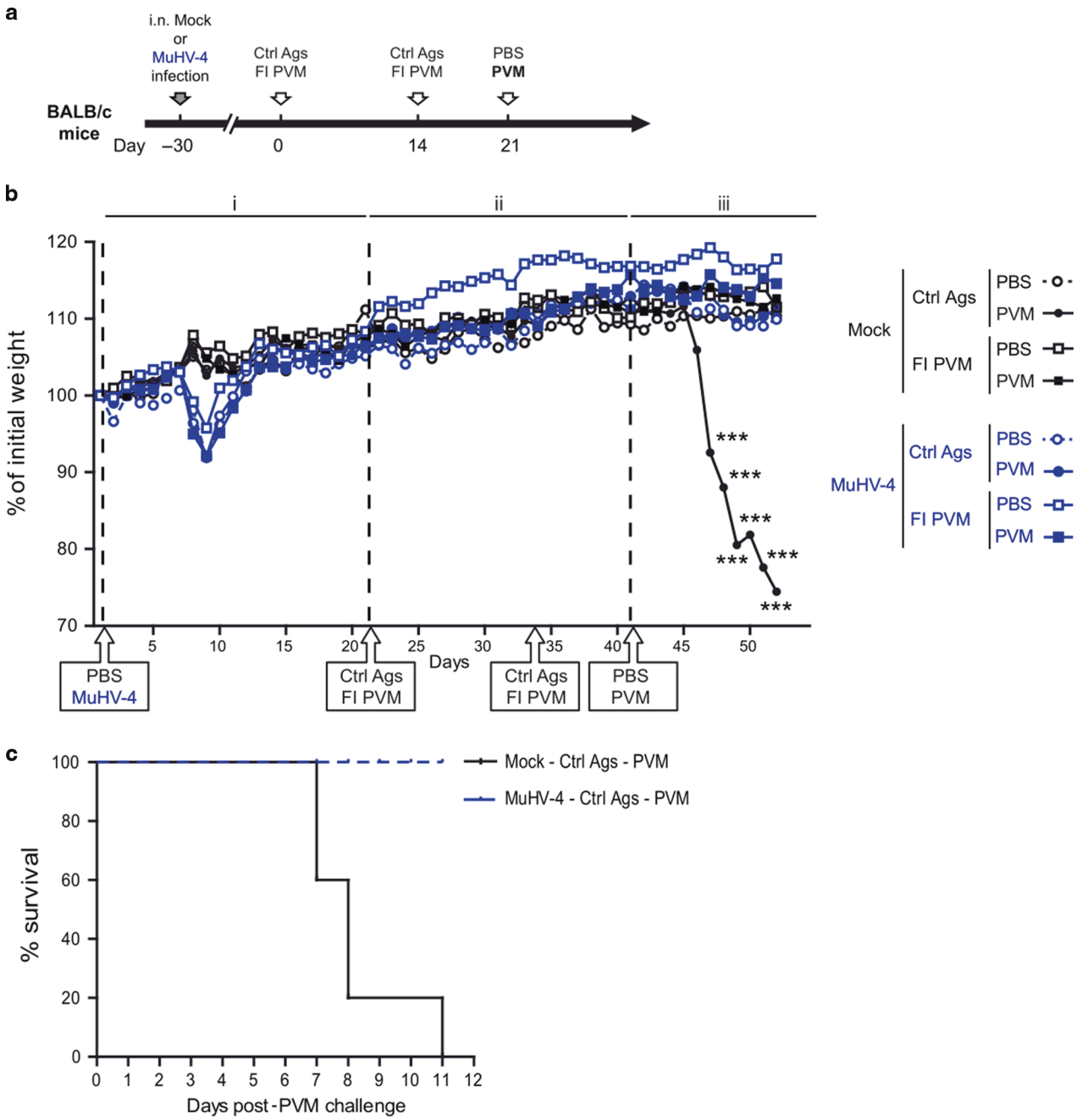

Fig. 2 MuHV-4 infection confers clinical protection against PVM primary infection. a–c Thirty days after i.n. Mock or MuHV-4 infection, BALB/c mice were vaccinated with FI-PVM Ags (or ctrl Ags), then challenged i.n. with $3{\cdot}10^2$ PFU of PVM (or PBS) and followed for weight evolution and clinical score. Experimental outline (**a**). Analysis of weight curves divided into three successive periods of interest: i, MuHV-4 infection; ii, FI-PVM vaccination; iii, PVM infection (**b**). Survival of Mock and MuHV-4-infected mice after PVM infection (**c**). Data are presented as means. ***$P \leq 0.001$ (one-way ANOVA and Bonferroni post-tests; only statistics for relevant comparisons are shown). Data are representative of at least three independent experiments with five mice per group.

infection does not affect PVM vaccine-induced sensitization through systemic effects but instead modulates the respiratory challenge.

To further confirm this hypothesis, we sensitized mice with PVM Ags before infecting them i.n. with MuHV-4 or PBS as control. One month later, mice were challenged i.n. with live PVM and the Th2 response was compared between groups (Fig. 4d). Although MuHV-4 lung infection occurred after the sensitization phase, it allowed significant inhibition of PVM vaccine-induced Th2 response upon respiratory challenge as revealed by the strong reduction of eosinophils (Fig. 4e) and the inhibition of type 2 histopathological features (Fig. 4f). Altogether, these findings indicate that MuHV-4 infection affects lung immunity and interferes with the challenge phase of PVM vaccine-induced immunopathology.

MuHV-4-trained AMs are not sufficient to inhibit PVM-induced immunopathologies

We have recently shown that MuHV-4 causes the long-term replacement of resident AMs by monocytes with regulatory functions.[11] In order to address the role of AMs from MuHV-4-infected mice in the context of PVM respiratory challenge, we

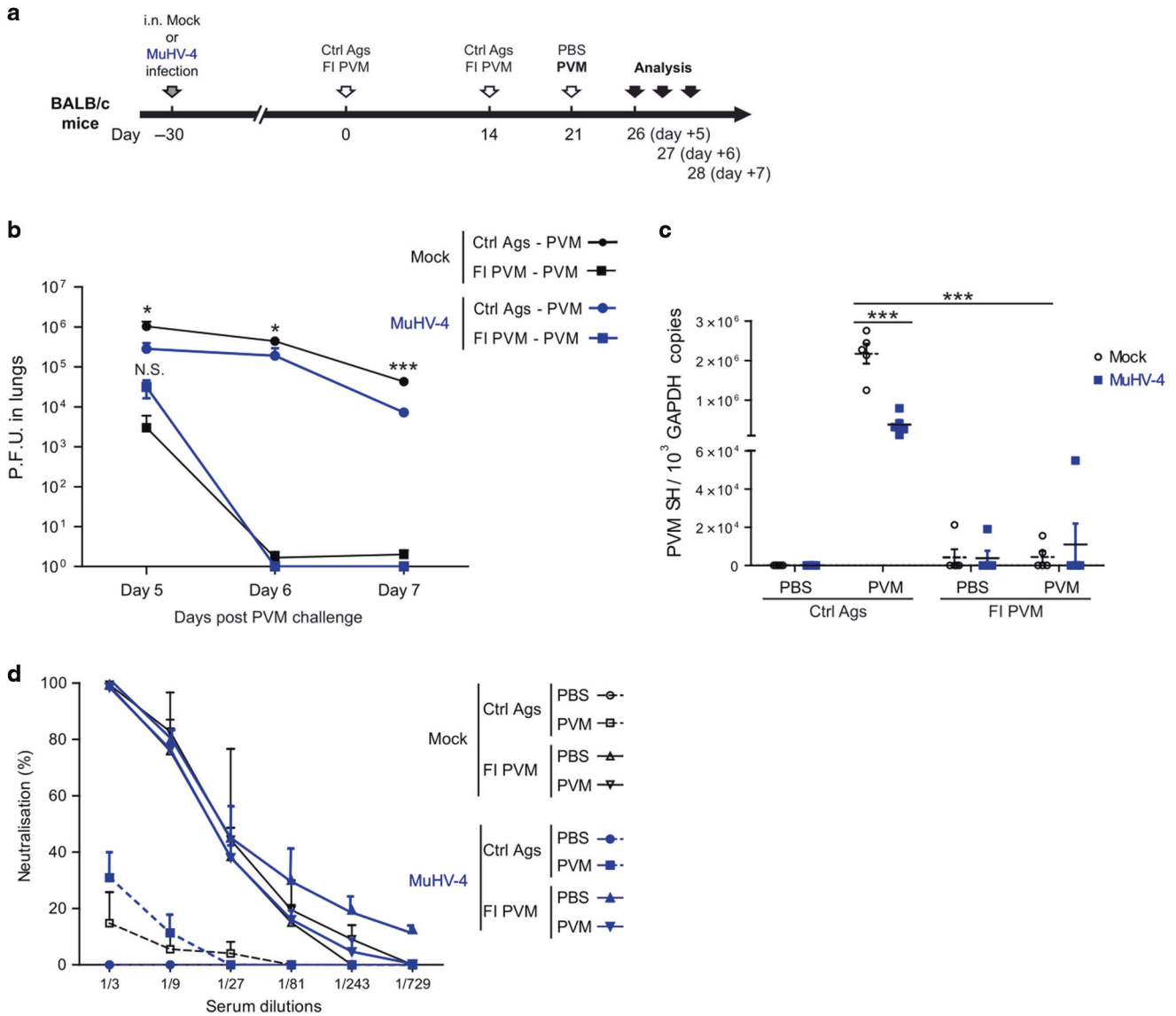

Fig. 3 MuHV-4 infection reduces lung PVM loads independently of the humoral response. a–d Thirty days after i.n. Mock or MuHV-4 infection, BALB/c mice were vaccinated with FI-PVM Ags (or Ctrl Ags), then challenged i.n. with $3{\cdot}10^2$ PFU of PVM (or PBS) and euthanized 5, 6 or 7 days later. Experimental outline (**a**). Infectious PVM virions in lungs at days 5, 6 and 7 after PVM i.n. challenge (**b**). PVM genomic copies in lungs at day 6 after PVM challenge. Statistics are highlighted for differences between Mock/Ctrl Ags/PVM and MuHV-4/Ctrl Ags/PVM groups. (**c**). Neutralisation of purified PVM virions by diluted sera from BALB/c mice euthanized at day 6 after PVM i.n. challenge (**d**). Data are presented as means ± SEM (and individual values in **c**). $*P \le 0.05$ and $***P \le 0.001$ (one-way ANOVA and Bonferroni post-tests). Data are representative of two independent experiments.

adoptively transferred AMs from Mock or MuHV-4-infected mice into naive recipient mice and submitted them either to PVM primo infection (Fig. 5a–c) or to PVM vaccine protocol (Fig. 5d, e). Despite the long-term engraftment of AMs from MuHV-4-infected mice and the persistence of their phenotypic changes (revealed by increased MHC-II expression), this adoptive transfer did not lead to any difference in comparison with mice receiving AMs from Mock-infected mice. Indeed, all mice succumbed to the PVM primary infection (Fig. 5a–c) or developed strong eosinophilia in case of PVM vaccine protocol (Fig. 5d, e), indicating that MuHV-4-trained AMs are not sufficient or are not directly associated with the protection against the PVM-induced immunopathologies.

Monocytes from MuHV-4-infected mice do not directly mediate the clinical protection against PVM pneumopathology

Beyond monocyte-derived AMs, newly recruited monocytes during PVM challenge could have a major effect in restricting PVM replication and/or in dampening inflammation. Notably, monocytes mobilized during acute MuHV-4 infection have been shown to exhibit regulatory properties such as secretion of high levels of IL-10[11]. First, we monitored monocytes infiltration in the airways during PVM-induced inflammation and observed massive recruitment of inflammatory monocytes at day 7 after primary PVM infection while no significant increase was observed in the context of type 2 response (Fig. 6a, b).

Second, we analyzed the phenotype of monocytes isolated at day 7 after PVM challenge from Mock or MuHV-4-infected mice (Fig. 6c–e). While we observed a significant upregulation of Sca-1 and IL-15Rα on Mock/PVM monocytes reflecting likely IFN-I signalling,[29,30] monocytes from MuHV-4/PVM group displayed a strong upregulation of MHC-II potentially associated with regulatory properties.[11,31] Intracellular stainings revealed an enhanced production of TNFα and iNOS by Mock/PVM monocytes compared with MuHV-4/PVM monocytes confirming the

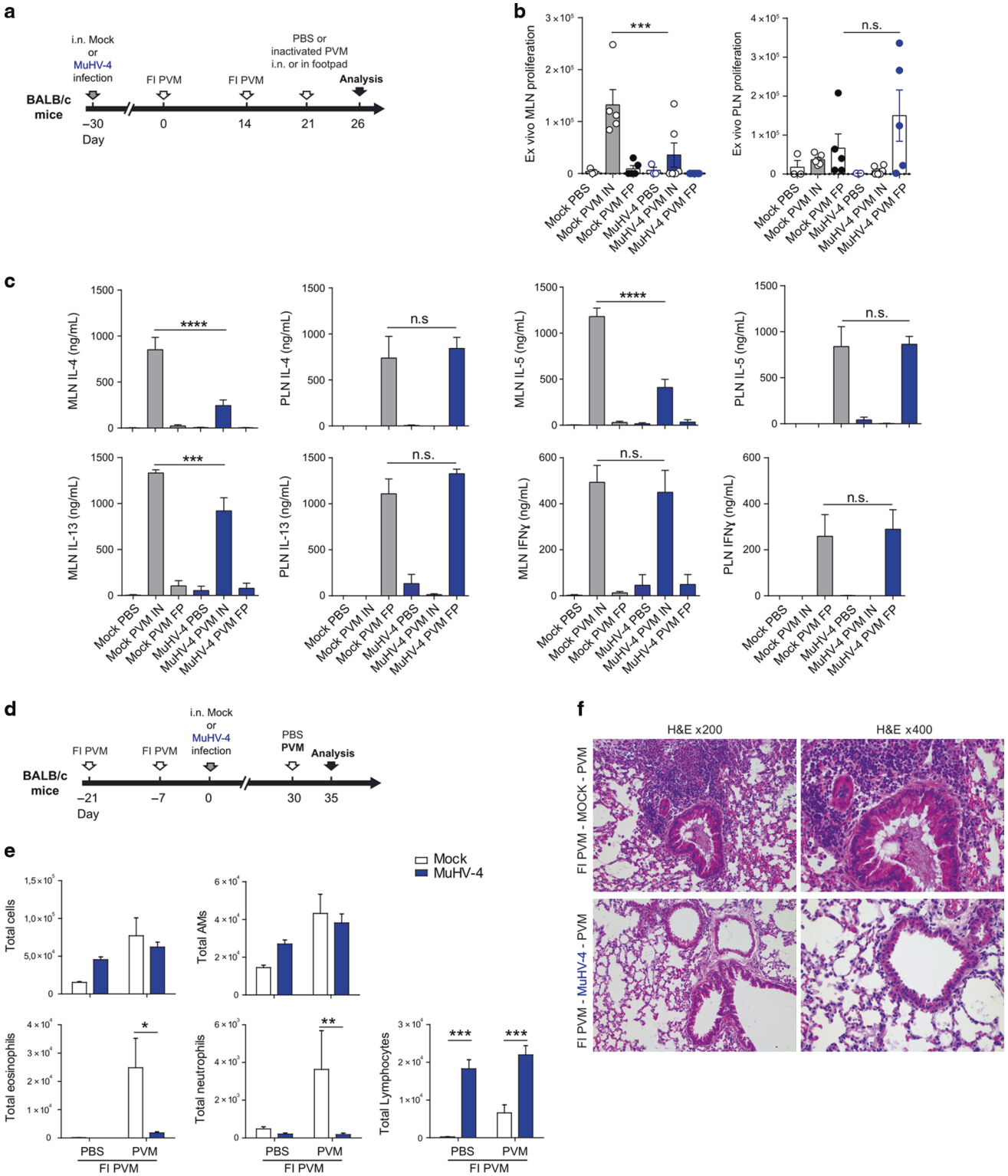

Fig. 4 MuHV-4 infection does not affect the PVM vaccine sensitization phase but significantly impairs the Th2 response upon PVM respiratory challenge. a–c Thirty days after i.n. Mock or MuHV-4 infection, BALB/c mice were vaccinated with FI-PVM Ags, then challenged i.n. or in footpad with the equivalent of $5{\cdot}10^4$ PFU of inactivated PVM virions (or PBS) before euthanasia 5 days later. Experimental outline (**a**). Ex vivo mediastinal lymph node (MLN) or popliteal lymph node (PLN) cells proliferation (**b**) and cytokine production (**c**) after restimulation for 48 h with heat-inactivated (HI) PVM Ags. **d–f** BALB/c mice were primary vaccinated (2 s.c. injections of 10 µg of FI-PVM Ags at 14-day intervals) then i.n. Mock or MuHV-4 infected and finally challenged i.n. 30 days later with $3{\cdot}10^2$ PFU of PVM (or PBS). Experimental outline (**d**). Absolute numbers of total leucocytes, of AMs, of lymphocytes, of eosinophils and of neutrophils in BALF (**e**). Histological analysis of lung sections stained with hematoxylin and eosin (H&E) (**f**). Data are presented as means ± SEM. $^{***}P \le 0.001$, $^{**}P \le 0.01$ and $^{*}P \le 0.05$ (one-way ANOVA and Bonferroni post-tests).

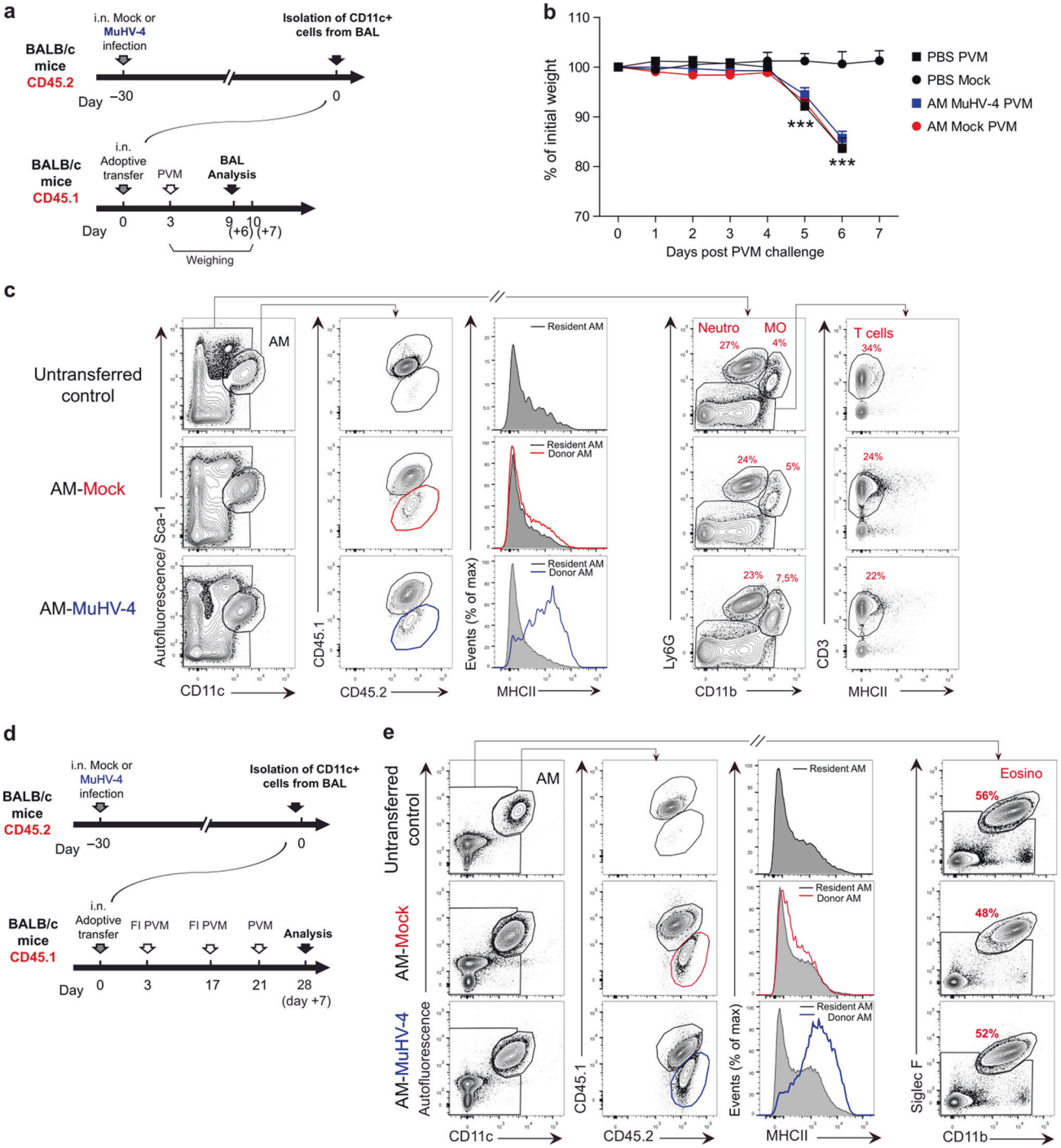

Fig. 5 MuHV4-trained AMs are not directly associated with the protection against PVM-induced immunopathologies. a–c Mock-infected CD45.1$^+$ recipient BALB/c mice received no AMs or were transferred i.n. with AMs purified from BALF of CD45.2$^+$ donor mice Mock infected or infected (for 30 days) i.n. with MuHV-4. Three days after cell transfer, recipient mice were infected i.n. with $3{\cdot}10^2$ PFU of PVM and were monitored for weight loss until euthanasia. Experimental outline (**a**). Evolution of weight (**b**). Flow cytometry (**c**) of cells from BALF (6 days after PVM intranasal challenge) to assess chimerism (CD45.1 vs CD45.2) of AMs (live CD45$^+$ autofluorescent CD11c$^+$); expression of MHC class II by resident and transferred AMs and proportion of BALF neutrophils (gated as live non-autofluorescent CD11c$^-$SSC^{int}CD11b$^+$Ly6G$^+$), monocytes (live non-autofluorescent CD11c$^-$CD11b$^+$Ly6G−Ly6C$^+$) and T cells (live non-autofluorescent CD11b$^-$Ly6G$^-$MHC-II$^-$CD3$^+$). **d**, **e** Mock-infected CD45.1$^+$ recipient BALB/c mice were transferred or not with AMs as described in (**a**) before being vaccinated by FI-PVM, then i.n. challenged with $3{\cdot}10^2$ PFU of PVM and euthanized 7 days later. Experimental outline (**d**). Flow cytometry of cells from BALF (**e**) to assess chimerism of AMs, expression of MHC class II by resident and transferred AMs as described in panel **c**, and, proportion of eosinophils (live non-autofluorescent CD11c$^-$SSC^{hi}CD11b^{int}SiglecF$^+$ in BALF).

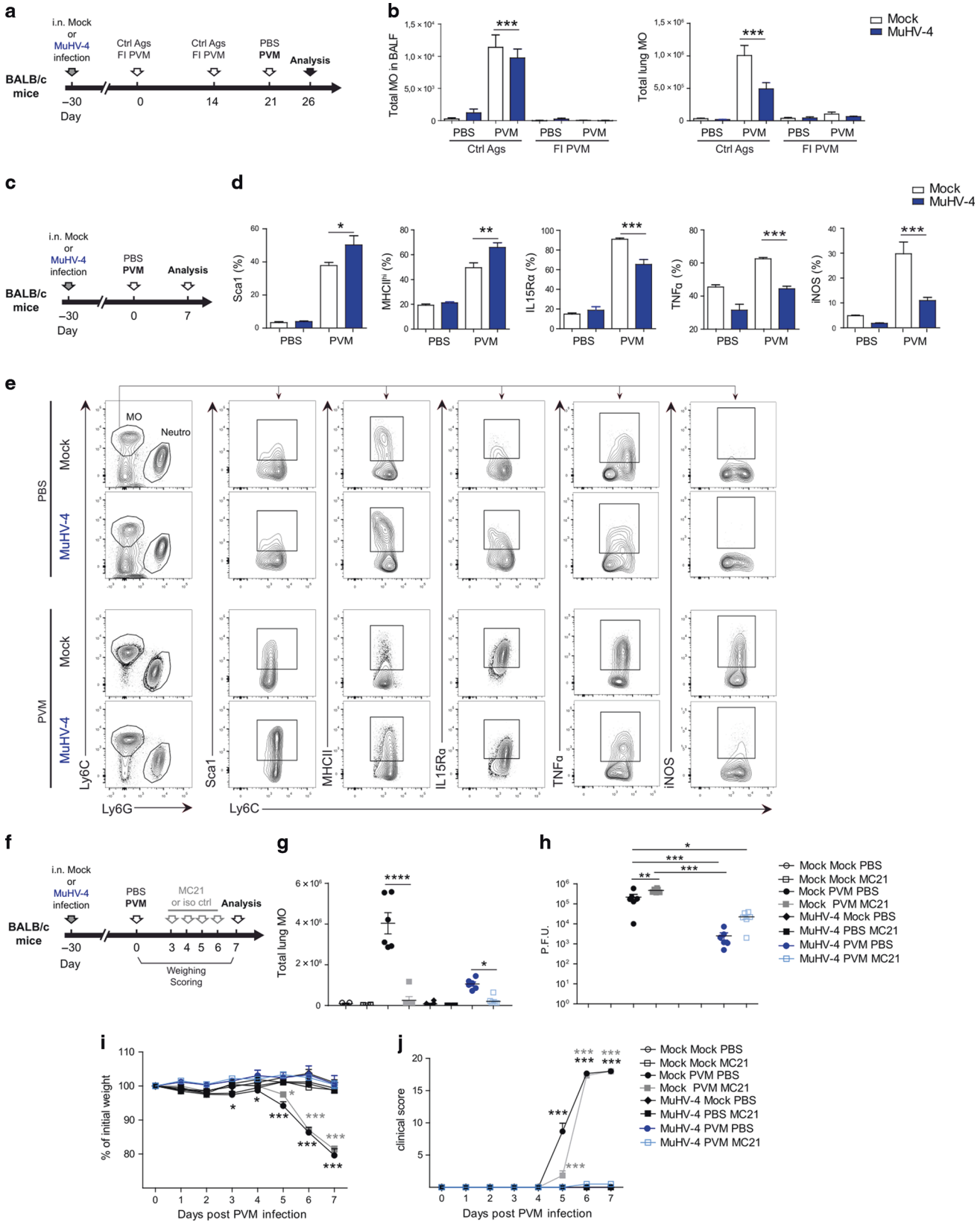

exacerbated pro-inflammatory profile of these cells in absence of previous MuHV-4 infection.

Finally, to investigate if monocytes are the main determinants of worsening (in Mock/PVM mice) or regulation (in MuHV-4/PVM mice) of inflammation after PVM infection, antibody-mediated depletion of CCR2+ cells was performed[32] from day 3 to day 7 after PVM challenge (Fig. 6f). Despite significant monocyte depletion (Fig. 6g), all Mock/PVM mice showed equivalent clinical

Fig. 6 Monocytes from MuHV-4-infected mice do not directly mediate clinical protection against PVM. a, **b** Thirty days after i.n. Mock or MuHV-4 infection, BALB/c mice were vaccinated with FI-PVM Ags (or ctrl Ags), then challenged i.n. with $3{\cdot}10^2$ PFU of PVM (or PBS) and euthanized 5 days later. Experimental outline (**a**). Flow cytometry quantification of monocytes in BALF and in lung (live $CD45^+$ non-autofluorescent $CD11c^-CD11b^+Ly6G^-Ly6C^+$) (**b**). **c–e** BALB/c mice were infected or not with MuHV-4, challenged i.n. 30 days later with $3{\cdot}10^2$ PFU of PVM (or PBS) and euthanized 7 days later. Experimental outline (**c**). Frequency of $Sca1^+$, MHC-II^{hi}, $IL15R\alpha^+$, $TNF\alpha^+$ or $iNOS^+$ lung monocytes (gated as in **b**) (**d**). Flow cytometry of lung cells pre-gated as neutrophils (live $CD45^+$ non-autofluorescent $CD11c^-SSC^{int}CD11b^+Ly6G^+$) or as monocytes (live $CD45^+$ non-autofluorescent $CD11c^-CD11b^+Ly6G^-Ly6C^+$) (**e**). **f–j** BALB/c mice were infected or not with MuHV-4, challenged i.n. 30 days later with $3{\cdot}10^2$ PFU of PVM (or PBS) and treated i.p. with anti-CCR2 depleting antibodies (20 µg) or isotype controls at days 3, 4, 5, 6 after PVM challenge. Experimental outline (**f**). Absolute numbers of lung monocytes (gated as in **b**) (**g**). Quantification of infectious PVM virions in lungs at day 7 after PVM challenge (**h**). Comparison of weight curves (**i**) and of clinical score (**j**) between groups. Data are presented as means ± SEM (**b**, **d**, **i**, **j**) or as means and individual values (**g–h**). ***$P \le 0.001$, **$P \le 0.01$ and *$P \le 0.05$ (one-way ANOVA and Bonferroni post-tests). The data are representative of two independent experiments.

signs and were all euthanized at day 7 for ethical reasons. By contrast, all MuHV-4-infected mice were fully protected against PVM immunopathology, regardless of the presence or not of monocytes (Fig. 6h–j). Accordingly, numbers of PVM plaque forming units (PFUs) in the lungs (Fig. 6h) were similar between depleted or not depleted mice but significantly reduced in MuHV-4 compared with Mock-infected mice. Thus, despite previous MuHV-4 priming, monocytes do not directly modulate immune defence against heterologous PVM infection.

MuHV-4 infection improves the effector CD8 response against PVM through MuHV-4 and PVM specific CD8 T cells

MuHV-4-infected mice display increased number of CD8 T cells in the airways (Fig. 1b). To characterize the response of these cells, we compared the phenotype of lung CD8 T cells isolated from Mock and MuHV-4-infected mice submitted to the PVM vaccine protocol or to the PVM primo-infection (Fig. 7a–c). This experiment revealed that MuHV-4 infection results in accumulation of lung memory CD8 T cells displaying an enhanced ability to produce IFNγ (Fig. 7b, c). In particular, MuHV-4/FI-PVM/PVM mice displayed the higher percentage of CD8 T cells producing IFNγ (Fig. 7b, c). It has been shown in other models that viral infections induce infiltration of lung memory CD8 T cells that contribute not only to immune defence against re-infection with the same virus,[33,34] but also against infection with unrelated viruses.[35] Therefore, to test the specificity of this better CD8 T cell response, we assessed MuHV-4 and PVM specific lung CD8 T cells response with H-2Kd-peptide tetramers (Fig. 7d, e). Interestingly, beside the expected presence of MuHV-4-specific CD8 T cells in all MuHV-4-infected mice, this experiment highlighted that MuHV-4/Ctrl Ags/PVM displayed a better CD8 response against PVM than corresponding mice non-infected by MuHV-4 (Fig. 7d, e). As expected, ex vivo restimulation of lung cells with either MuHV-4 or PVM peptides (Fig. 7f, g) identified MuHV-4-specific CD8 T cells in MuHV-4-infected mice and PVM-specific CD8 T cells in PVM-infected mice. Strikingly, higher numbers of $IFN\gamma^+$ CD8 T cells were observed in MuHV-4/Ctrl Ags/PVM after restimulation with either MuHV-4 or PVM peptides (Fig. 7f, g). These results highlight therefore that MuHV-4 infection induces the presence of MuHV-4 specific memory CD8 T cells. Importantly, it also shows that, upon PVM heterologous challenge, more PVM-specific CD8 T cells are observed in MuHV-4-infected mice. Finally, both MuHV-4 and PVM peptides induce higher numbers of $IFN\gamma^+$ CD8 T cells in MuHV-4/Ctrl Ags/PVM mice.

To further investigate whether the MuHV-4-enhanced CD8 T cells response is necessary for the protection against PVM-induced pneumopathologies, we treated mice with anti-CD8 depleting antibodies at PVM challenge (Fig. 8a–i). While this protocol only partially depleted lung CD8 T cells (Fig. 8b, f), it profoundly affected PVM-induced immunopathologies. Indeed, CD8 T cells depletion impaired the capacity of MuHV-4 infection to protect against pneumovirus vaccine-related Th2 hypersensitivity (Fig. 8c, d). Similarly, depletion of these cells reduced the capacity of MuHV-4-infected mice to control PVM replication and markedly increased weight loss and clinical score of these mice (Fig. 8g–i). Finally, in order to test if lung CD8 T cells from MuHV-4-infected mice are sufficient for the protection against PVM-induced pneumopathologies, we adoptively transferred lung CD8 T cells isolated from mice infected by MuHV-4 for 1 month to recipient mice previously vaccinated with FI-PVM or control Ags. One day after transfer, these mice were infected with PVM (Fig. 8j–n). While CD8 T cells from MuHV-4-infected mice did not prevent from lung eosinophilia in the PVM vaccine-induced immunopathology, they provided protection against PVM infection in non-vaccinated mice as revealed by the absence of weight loss and pulmonary neutrophilia (Fig. 8m, n).

Altogether, these results demonstrate that the MuHV-4 enhanced CD8 T cells response is required for protection of MuHV-4-infected mice against both PVM-induced immunopathologies. Moreover, these cells are sufficient to mediate protection against the PVM-induced disease in non-vaccinated mice.

DISCUSSION

There is considerable variation in disease susceptibility between individuals. While genetic factors account for at most 50% of the immune variation, environment, and especially symbiotic and pathogenic microorganisms, appears to be the main determinant of immunological diversity.[10,36] This diversity is particularly observed for RSV infections in children and ranges from mild symptoms to severe pneumopathology requiring hospitalization.[37] While RSV-induced immunopathologies are not yet well defined, identification of key environmental factors shaping these responses could contribute to develop new prevention approaches and therapies. In this study, we examined how the immunological environment of a previous γHV infection impacts the development of pneumovirus-induced diseases. We found that MuHV-4 infection strongly attenuates Th2 PVM vaccine-enhanced disease without preventing the development of an anti-PVM vaccine immunity. Moreover, we also observed that previous MuHV-4 infection confers clinical protection against heterologous PVM infection which is otherwise lethal. In both cases, CD8 T cells appeared to be central to this protection.

The FI-PVM vaccine used in this study was prepared similarly to the RSV "lot 100" vaccine tested in the early 1960s. This vaccine led to the development of severe respiratory complications when vaccinated children subsequently encountered natural RSV infection (80% had to be hospitalized with 2 death cases).[3] Several decades later, there is yet no licensed RSV vaccine despite 50 years of effort to understand the pathogenesis of this vaccine-enhanced disease and to develop new vaccine approaches.[38] Here, we showed that while FI-PVM vaccine induced a similar neutralizing antibody response in both Mock and MuHV-4-infected mice (Fig. 3), MuHV-4 infection completely protected against vaccine-mediated Th2 immunopathology (Fig. 1). Moreover, protection was also observed when MuHV-4 infection occurred after FI-PVM vaccination (Fig. 4). This therefore suggests that the immune environment in which infectious pneumovirus challenge is encountered is of major importance and not the immune

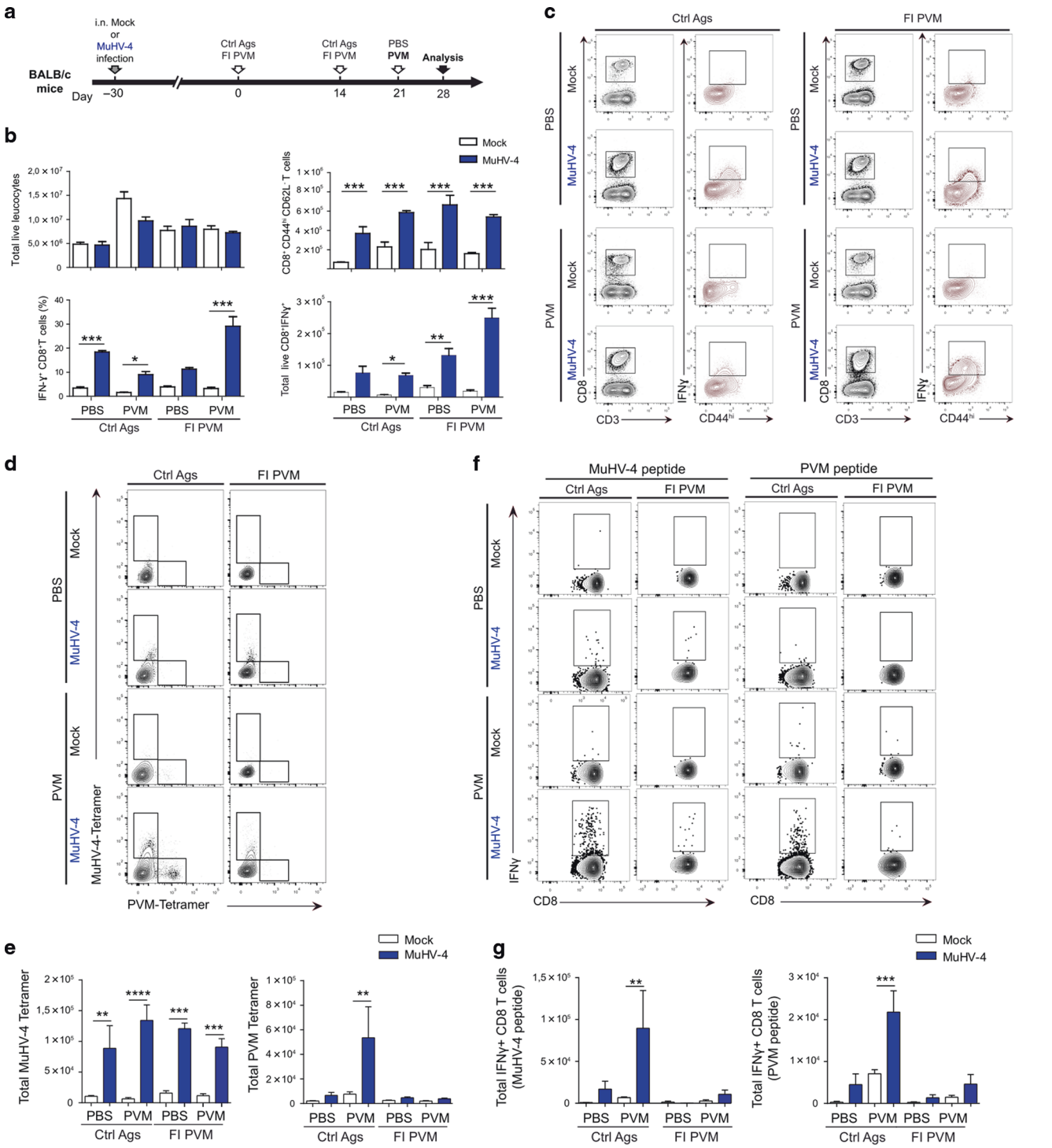

Fig. 7 MuHV-4 infection improves the effector CD8 T cells response against PVM. a–g Thirty days after i.n. Mock or MuHV-4 infection, BALB/c mice were vaccinated with FI-PVM. Ags (or ctrl Ags), then challenged i.n. with $3{\cdot}10^2$ PFU of PVM (or PBS) and euthanized 7 days later. Experimental outline (**a**). Absolute numbers of total lung leucocytes (live $CD45^+$) and effector memory T cells (live $CD45^+$ non-autofluorescent $CD11c^-CD11b^-CD3^+CD8^+CD62L^-CD44^{hi}$); frequency and absolute numbers of $IFN\gamma^+$ effector memory T cells after restimulation with PMA and ionomycin during 4 h before intracellular staining (**b**). Representative flow dot plots of CD8 T cells and $IFN\gamma^+$ CD8 T cells (live $CD45^+$ non-autofluorescent $CD11c^-CD11b^-CD3^+CD8^+CD62L^-CD44^{hi}$) (**c**). Representative flow dot plots (**d**) and total numbers (**e**) of MuHV-4 specific $ORF65^{131-140}$ H-2Kd tetramer and PVM specific $P^{261-270}$ H-2Kd tetramer stainings of lung cells 7 days after PVM challenge. Representative flow dot plots (**f**) and total numbers (**g**) of lung $IFN\gamma^+$ CD8 T cells (live $CD45^+$ non-autofluorescent $CD11c^-CD11b^-CD3^+CD8^+CD62L^-CD44^{hi}$) after restimulation with MuHV-4 specific peptides ($M2^{91-99}$ and $ORF65^{131-140}$) or with PVM specific peptides ($P^{261-269}$ and $F^{304-313}$) during 4 h before intracellular staining. Data are presented as means ± SEM. $^*P \le 0.05$; $^{**}P \le 0.01$ and $^{***}P \le 0.001$ (one-way ANOVA and Bonferroni post-tests). Data are representative of two independent experiments.

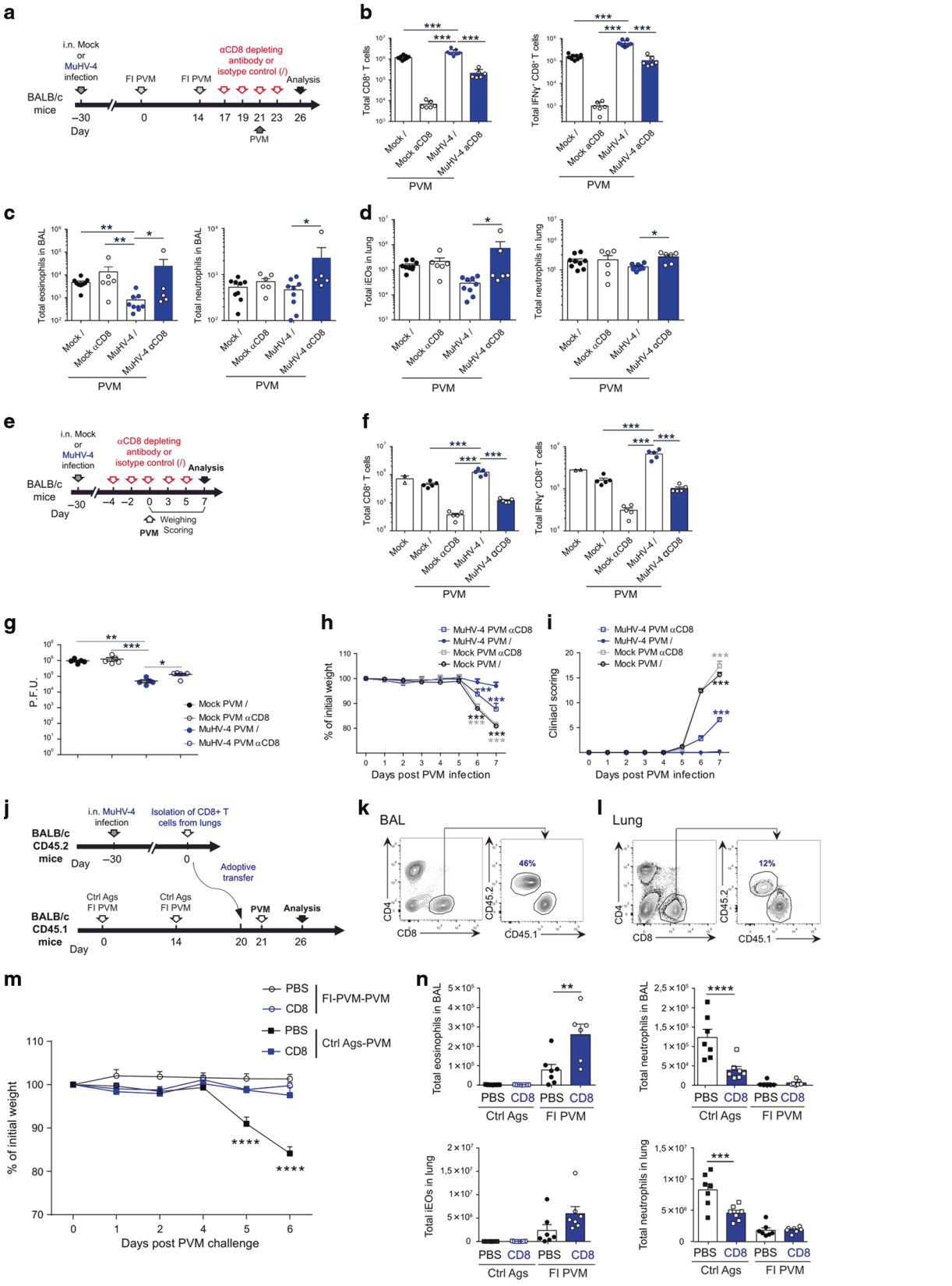

environment in which the vaccine is administered. These results obtained with MuHV-4 can be paralleled with the fact that previous immunity to influenza virus protects from the immunopathology induced by an RSV attachment protein vaccine.[39] These observations could help us rethinking the cause of this immunopathology and to develop new prevention approaches against pneumoviruses based on the education of the lung microenvironment.

Fig. 8 CD8 T cells infiltrating the lung after MuHV-4 infection are necessary and sufficient to protect from PVM primary infection. a–d BALB/c mice were infected or not with MuHV-4, submitted to PVM vaccination, challenged i.n. 30 days later with $3{\cdot}10^2$ PFU of PVM and treated i.p. with anti-CD8 depleting antibodies (100 µg) or isotype controls at days −4, −2, 0, and 2 after PVM i.n. challenge. Mice were euthanized at day 5 after PVM challenge. Experimental outline (**a**). Absolute numbers of effector memory CD8 T cells and of IFNγ + effector memory CD8 T cells in lungs (live $CD45^+$ non-autofluorescent $CD11c^-CD11b^-CD3^+CD8$) (**b**). Absolute numbers of eosinophils (live non-autofluorescent $SSC^{hi}CD11b^{int}SiglecF^+$), and of neutrophils (live non-autofluorescent $CD11c^-SSC^{int}CD11b^+Ly6G^+$) in BALF (**c**) or in lung (**d**). **(e–i)** BALB/c mice were infected or not with MuHV-4, challenged i.n. 30 days later with $3{\cdot}10^2$ PFU of PVM, and treated i.p. with anti-CD8-depleting antibodies (100 µg) or isotype controls at days −4, −2, 0, 3, 5 after PVM i.n. challenge. Mice were euthanized at day 7 after PVM challenge. Experimental outline (**e**). Absolute numbers of effector memory CD8 T cells and of $IFN\gamma^+$ CD8 T cells in lungs (live $CD45^+$ non-autofluorescent $CD11c^-CD11b^-CD3^+CD8^+CD62L^-CD44^{hi}$) (**f**). Quantification of infectious PVM virions in lungs (**g**). Comparison of weight curves (**h**) and of clinical score (**i**) between groups. (**j–n**) CD8 T cells were purified from CD45.2+ BALB/c mice infected for 1 month with MuHV-4 and adoptively transferred into Mock CD45.1 BALB/c mice previously submitted or not to the FI-PVM vaccine protocol. Recipient mice were then challenged i.n. with $3{\cdot}10^2$ PFU of PVM and euthanized 6 days later. Experimental outline (**j**). Representative flow plots of $CD45.1^+$ and $CD45.2^+$ CD8 T cells (live $CD45^+$non-autofluorescent $CD11c^-CD11b^-CD3^+CD8^+$) isolated from BALF (**k**) and lung (**l**) of PVM challenged recipient mice. Comparison of weight curves between groups (**m**). Absolute numbers of BALF and lung eosinophils (gated as in **c**, **d**) (**n**).

This immune environment appeared also to be important in the context of PVM primary infection as it determined the nature of the inflammation and survival of the mice (Figs. 1 and 2). The influence of other microorganisms on lung microenvironment and on subsequent pneumovirus infections had already been described. Thus, oral supplementation with *Lactobacillus johnsonii* mediates airway mucosal protection through immunomodulatory metabolites and altered function of immune cells such as dendritic cells.[40] These results remind also the concept of heterologous anti-viral immunity that takes into account the influence that immune responses to one virus can have on that of another.[41,42]

Here, we showed that MuHV-4 infection induced a long-term infiltration of CD8 T cells in the lung, capable to express protective effector functions in response to heterologous challenge (Fig. 7). These results are in contrast with many studies on RSV infection in mice that have shown that RSV-specific CD8 T cells are involved in immunopathology leading to exacerbated morbidity and mortality.[43–48] In that context, it is important to note that RSV replication in mice differs from infection in humans and the model also lacks several pathological features of RSV natural infection in infants, including the predominance of neutrophils in airway exudates and the extensive bronchiolar epithelial destruction.[49] The use of PVM in mice allows us to assess the potential involvement of CD8 T cells in a natural host–pathogen relationship. Interestingly, we showed that lung MuHV-4 experienced CD8 T cells play a crucial role in the provided protection against both PVM-induced immunopathologies. Indeed, CD8 T cells infiltrating the lung after MuHV-4 infection appeared to be necessary (Fig. 8e–i) and sufficient (Fig. 8j–n) to inhibit the PVM primary pathology. In contrast, they were required (Fig. 8a–d) but unable to protect alone (Fig. 8j–n) from the Th2 PVM vaccine-enhanced disease. This absence of protection could be related to this particular experimental design but could also reveal that other partners are required in that context.

Another question was related to the mode of activation and to the specificity of these CD8 T cells. We first showed that MuHV-4 infected mice display more effector memory CD8 T cells in the lung than their Mock-infected counterparts (Fig. 7b, c). Interestingly, these cells appeared to be more reactive to ex vivo non-specific restimulation (Fig. 7b, c). This therefore suggest that, in vivo, these effector memory CD8 T cells could be easily activated upon PVM challenge through TCR-independent bystander activation as described.[50,51] Second, a large proportion of these cells is likely MuHV-4 specific as revealed by tetramer staining (Fig. 7d, e). Interestingly, after PVM superinfection, these cells responded better to ex vivo restimulation with MuHV-4 peptide suggesting here also some degree of pre-activation by this heterologous PVM infection (Fig. 7f, g). Importantly, these MuHV-4-experienced CD8 T cells were sufficient to confer complete protection against PVM infection (Fig. 8j–n). Finally, MuHV-4 infected mice developed also a better specific CD8 response against PVM as revealed by PVM-specific tetramer staining (Fig. 7d, e) and ex vivo restimulation with a PVM peptide (Fig. 7f, g). This observation could be explained by an indirect role of these MuHV-4 experienced CD8 T cells in triggering recruitment and/or activation of other immune players.[52] Similarly to what has been shown in other models,[53] these CD8 T cells producing IFNγ could act as "helper" cells, supporting the ability of dendritic cells to produce cytokines such as interleukin-12 (IL-12) p70 and promoting therefore specific heterologous CD8 response against PVM. This relationship will have to be studied in the future. These CD8 T cells could also have a regulatory phenotype as already observed after MuHV-4 infection.[54] Accordingly, in the PVM primary infection model, we observed a significant production of IL-10 in the BAL (Fig. 1i) suggesting that these CD8 T cells could mediate protection through immunomodulatory effects. Further experiments will have to be performed to distinguish between an improved viral clearance and regulation of immunopathology or both. Finally, we have recently shown that MuHV-4 protects against allergic asthma by inducing the long-term replacement of resident AMs with regulatory monocytes.[11] As monocytes are also recruited during primary PVM infection (Fig. 6), we hypothesized that monocytes from MuHV-4-infected mice, primed for regulatory functions, could prevent development of PVM-induced immunopathology. In contrast, in Mock-infected mice, monocytes could trigger or reinforce deleterious inflammation upon PVM infection. However, depletion of monocytes during PVM i.n. infection did not lead to any difference in clinical signs nor in control of viral burden. While this result has allowed ruling out a direct influence of pre-educated monocytes on the outcome of PVM challenge, it did not exclude a potential importance of monocytes, recruited during the acute phase of MuHV-4 infection, in educating lung CD8 T cells for long-term enhanced cytotoxic capacities. Crosstalk between monocytes and lung infiltrating CD8 T cells following MuHV-4 infection will therefore need to be investigated more deeply.

Similarly, CD8 T cell homing to the respiratory mucosa after adenovirus infection has been shown to induce long-lasting modifications on AMs, beneficial to host defence against bacterial superinfection.[55] Here, adoptive transfer of AMs from MuHV-4 infected mice was not sufficient to prevent PVM-induced immunopathologies (Fig. 5). However, host resident AMs, not affected by MuHV-4, were still present and could have supported active PVM replication,[56] eliciting the release of pro-inflammatory mediators[57] such as IL-6.[28] It could be worthwhile in the future to distinguish between the potential deleterious impact of the host AMs during PVM acute infection and the regulatory role of MuHV-4-trained AMs,[11] and to decipher the role of CD8 T cells in that context.[55]

Altogether, our results have shown that previous γHV infection induce a profound immunomodulation allowing protection of the host from pneumovirus-induced diseases. CD8 T cells appeared to play a central role in this protection. These results open

perspectives for vaccination against pneumoviruses and highlight that some so-called pathogens could be revealed as beneficial for their host.

METHODS

Mice

Female BALB/c mice (Envigo, Venray, The Netherlands) were housed according to the guidelines of the European Convention for the Protection of Vertebrate Animals used for Experimental and other Scientific Purposes (CETS no. 123). The protocol was approved by the Committee on the Ethics of Animal Experiments of the University of Liege (Permit nos. 1367 and 1706). Mice were used at 7–8 weeks of age and were randomly assigned to the various groups.

Cells

BHK-21 fibroblasts (ATCC CCL-10) and Raw 264.7 (ATCC TIB-71) were grown in DMEM supplemented with 2 mM glutamine, 100 U penicillin/mL, 100 mg streptomycin/mL and 10% FCS.

Viruses

The wild type MHV-68 strain of MuHV-4 was grown on BHK cells and was purified and titrated as described.[11] The highly pathogenic strain J3666 of PVM was maintained via continuous in vivo passages. Stocks were produced in vitro in BHK-21 cells at 32 °C, concentrated and purified (sucrose cushion and tartrate gradient as decribed[11]). Infectious PVM particles were quantified by plaque assay in BHK-21 cells.

Mouse infections and challenge with inactivated PVM

I.n. infections (in 50 µl of PBS) were performed under isoflurane anaesthesia with $1{\cdot}10^4$ PFU in the case of MuHV-4 and with $3{\cdot}10^2$ PFU in the case of PVM. Mock-infected mice received 50 µl of PBS. For the inactivated PVM challenge, mice received the equivalent of 5.10^4 PFU of PVM inactivated in 0.1% Triton X-100 for 3 h at 4 °C.

PVM vaccine preparation and administration

FI-PVM Ags were prepared as described.[16] RAW 264.7 cell line were inoculated with PVM at a multiplicity of infection of 0.05. Ninety-six hours after infection, the cells were scraped and sonicated to release cell-associated virions. Infected-cell debris were removed by low-speed centrifugation ($1000 \times g$, 20 min) and formalin was added (1/3000) to the clarified supernatants for 48 h at 37 °C. FI-PVM were collected by ultracentrifugation ($100{,}000 \times g$, 2 h), washed twice with cold PBS and finally resuspended in PBS. Protein concentration was determined by Bradford assay. Ctrl Ags were produced similarly from parallel cultures of uninfected RAW 264.7 cells. The loss of infectivity was confirmed by plaque assay. Isoflurane anesthetized mice were inoculated subcutaneously (s.c.) on days 0 and 14 with either 100 µl containing 10 µg FI-PVM in alum adjuvant (Pierce Biotechnology), Ags/alum ratio 3/1, or with 100 µL Ctrl Ags with alum in parallel.

Clinical evaluation

The clinical scoring was performed in accordance with the evaluation grids provided by the local ethical commission. Mice were assessed daily for weight loss and clinical symptoms. In particular, different parameters were monitored: activity, posture, gait, coat, type of respiration, state of activity, and deshydratation. Excessive loss of body weight (>25%) or obvious sign of suffering were considered as limit points in the experiments.

ELISA, quantitative PCR, and measurement of PVM viral loads

Quantification of MuHV-4 specific antibodies by ELISA and quantification of MuHV-4 genomic and cellular DNA copies by quantitative PCR were performed as described.[58] PVM genomes from lung tissue were measured by quantitative RT-PCR with dual standard curve as previously described.[16] Infectious PVM loads at euthanasia were quantified by plaque assay from co-culture of lung homogenate dilutions with BHK-21 permissive cells.

Anti-PVM neutralisation assay

Serum was serially diluted (1/3 to 1/729) in DMEM. PVM virions (100 PFU) were incubated at 37 °C for 2 h with 200 µL of each serum dilution. Samples were then titrated on BHK-21 cells.

BAL, cytology, and cytokine measurement

After euthanasia, the trachea was catheterized and BAL was performed by two consecutive flushes of the lungs with 1 ml of ice-cold PBS containing EDTA and protease inhibitors. Cell density in BALF was determined using a hemocytometer after Tuerk solution staining (Sigma-Aldrich). Differential cell counts in BALF were determined by flow cytometry. Concentrations of BALF cytokines were measured by ELISA (Ready-SET-Go, eBioscience).

Lung histology

Lungs were fixed in 5% formalin, paraffin embedded and cut into 5-µm sections that were then stained with hematoxylin-eosin before analysis.

Preparations of cell suspension from organs

To harvest lung cells, mice were perfused with ice-cold PBS through the right ventricle. Lung lobes were then collected into HBSS medium containing 1 mg/ml collagenase D (Roche) and 50 µg/ml DNase I (Roche), processed with a gentleMACS dissociator (Miltenyi) and incubated for 30 min at 37 °C. Cell suspensions were finally washed and treated with erythrocytes lysis buffer (eBioscience). For MLN and PLN cells, LNs were harvested, and single-cell suspensions were prepared using a sterile syringe plunger. For all preparations, cells were finally strained through a 70 µm filter.

Restimulation of MLN and PLN cells

A total of $2{\cdot}10^5$ LN cells were cultured in a 96-well plate in RPMI medium supplemented with 2 mM glutamine, 100 U penicillin/mL, 100 mg streptomycin/mL, 10% FCS and 50 µM β-mercaptoethanol, with or without heat-inactivated (HI)-PVM (equivalent of $2{\cdot}10^5$ PFU inactivated by incubation during 30 min at 70°). After a 4-day culture at 37 °C, total cells were counted to estimate proliferation and culture supernatants were assayed for IL-4, IL-5, IL-13 and IFN-ɣ by ELISA (Ready-SET-Go, eBioscience). For restimulation with peptides, cells were stimulated with MuHV-4 specific peptides ($M2^{91-99}$ and $ORF65^{131-140}$) or with PVM-specific peptides ($P^{261-269}$ and $F^{304-313}$) at 37 °C during 4 h before intracellular staining.

Flow cytometry

Labelling of cells was performed at 4° in FACS buffer (PBS containing 0.5% BSA, 2 mM EDTA and 0,01% sodium azide). Cells were first incubated for 20 min with a purified rat anti-mouse CD16/CD32 (eBioscience) to block Fc binding. Multicolour staining was performed for 30 min by using various panels of fluorochrome-conjugated antibodies: antibodies to CD45 (30-F11, BV510 or PE-Cy7), MHC-II (M5/114.15.2, PE-Cy7 or efluor 450), CD3e (145-2C11, APC-Cy7, APC or PE), CD8 (53-6.7, AlexaFluor488, APC or PE), CD4 (RM 4-5, PerCP-Cy5.5 or APC), CD19 (MB19-1, APC-Cy7), Ly6G (1A8, APC-Cy7 or APC), SiglecF (E50-2440, Alexa-Fluor647 or PE), CD11b (M1/70, APC-eFluor780 or BV711), CD11c (N418, PerCP-Cy5.5 or AlexaFluor700), Ly6C (HK1.4, BV785 or PE-Cy7), and Ly6A/E (D7, FITC), CD215 (DNT15Rα, PE), CD44 (IM7, PE-cy7), CD62L (MEL-14, FITC), CD45.1 (A20, APC), CD45.2 (1O4, V500) from BioLegend or from BD Biosciences and antibody to CCR2 (475301, PE), from R&D Systems. Dead cells were stained using Fixable Viability Stain 510 (0.4 µg ml^{-1}, BD Bioscience,) or Fixable Viability Dye eFluor780 (1000× dilution, eBioscience). For intracellular cytokine staining, cells were cultured at 37 °C in RPMI

medium complemented with 2 mM glutamine, 100 U penicillin ml^{-1}, 100 mg streptomycin ml^{-1} and 5% FCS for 4 h in the presence of brefeldin A (10 µg mL^{-1}, eBioscience), monensin (2 µM, eBioscience), and restimulating agent. To achieve unspecific restimulation, cells were incubated with phorbol 12-myristate 13-acetate (PMA, 20 ng mL^{-1}, Sigma-Adlrich) and ionomycin (1 µg mL^{-1}, Sigma-Adlrich). Following surface and viability stainings, cells were fixed in 2% paraformaldehyde overnight and washed with permeabilization buffer (eBioscience) before being incubated with antibodies against IFN-γ (clone XMG1.2, PE, BioLegend), TNFα (MP6-XT22, BV711, BioLegend) or NOS2 (CXNFT, PE, eBioscience), in permeabilization Buffer for 20 min at 4 °C. For intranuclear staining for transcription factors, cells were fixed and permeabilized using Foxp3/Transcription factor staining buffer set (eBioscience) following the manufacturer's instruction and incubated 20 min at 4 °C with antibody against either GATA-3 (TWAJ, PE) or FoxP3 (FJK-16s, eFluor 450) from eBioscience diluted in permeabilization buffer. All samples were processed on a BD LSR Fortessa X-20, equipped with 50-mW violet 405-nm, 50-mW blue 488-nm, 50-mW yellow–green 561-nm and 40-mW red 633-nm lasers. Data were analyzed with FlowJo v10 (Treestar).

Tetramer staining

MHC/peptide tetramers for MuHV-4 ORF65$^{131–140}$ H-2Kd and PVM P$^{261–270}$ H-2Kd epitopes, conjugated to phycoerythrin and allophycocyanin respectively were obtained from the National Institutes of Health Tetramer Core Facility (Emory University, Atlanta, GA). Lung cells were stained with tetramers for 30 min at RT and further stained with antibodies against surface markers as described above.

AM and CD8 isolation and transfer

AMs were purified by positive CD11c MACS selection (Miltenyi Biotech), according to the manufacturer's protocol, from BALF of mock or MuHV-4 infected mice 30 days after infection. AM purity was checked by flow cytometry (autofluorescent $CD11c^+$ living cells) and was confirmed to be >95%. For transfer experiments, 8×10^5 AMs in 75 µl of PBS were injected i.n. into naive $CD45.1^+$ congenic BALB/c mice under isoflurane anesthesia. Three days after AM transfer, recipient mice were superinfected with PVM or vaccinated with FI-PVM twice and superinfected with PVM as described in Fig. 5.

CD8 T cells were purified by negative CD8 MACS selection (Miltenyi Biotech), according to the manufacturer's protocol, from lung of $CD45.2^+$ mice infected with MuHV-4 for 30 days. CD8 T cells purity was checked by flow cytometry (non-autofluorescent $CD45^+CD11c^-CD3^+CD8^+$ living cells) and was confirmed to be >90%. A total of 10^6 CD8s in 75 µl of PBS were injected i.n. under isoflurane anesthesia into naive $CD45.1^+$ congenic BALB/c mice that have been previously submitted or not to FI-PVM vaccine protocol. One day after CD8 transfer, recipient mice were superinfected with PVM as described in Fig. 8.

In vivo antibody treatments and monocyte or CD8 depletion

For monocyte depletion, α-CCR2 antibody (clone MC21, 20 µg/dose in 200 µL PBS, i.p.) was administered for 5 consecutive days. A similar concentration of rat IgG was used as a control antibody. CD8 T cells were depleted by treating mice with an α-CD8 antibody (clone YTS 169.4, 100 µg/dose in 200 µL PBS, i.p.) 4 or 5 times every other days. Control mice received rat IgG at a similar concentration at the indicated time points.

Statistical analysis

Each experiment was repeated at least two times, $n \geq 5$ in each experimental group. Data were presented as individual values or means ± SEM. The differences between mean values were calculated by the use of ANOVA-1 followed by Bonferroni post-test. p values ≤ 0.05 were considered as statistically significant.

ACKNOWLEDGEMENTS

This work was Supported by the University of Liège (VIR-IMPRINT ARC), "Fonds de la Recherche Scientifique - Fonds National Belge de la Recherche Scientifique" F.R.S./FNRS ("credit de recherche" J007515F; "projet de recherche" T.0195.16; research associate support for B.G.D.; postdoctoral researcher for B.M. and research fellow for M.D. and C.M.), Institut MERIEUX (starting grant to L.G.), the EOS joint programme of F.R.S./FNRS and Fonds wetenschapellijk onderzoek – Vlaanderen - FWO (EOS ID: 30981113). B.M. is supported by an ERC Starting Grant (ERC-StG-2020 VIROME, ID: 853608). The authors thank the technician and administrative team of the Immunology-Vaccinology lab for very helpful assistance.

AUTHOR CONTRIBUTIONS

L.G., B.M. and M.D. designed the experiments. M.D., B.M., J.J. and C.M. did most of the experiments and compiled the data. L.G., B.M., M.D., C.M., G.G., D.D. and B.D. analyzed the data; L.G., B.M., and M.D. prepared the figures; L.G., B.M. and M.D. wrote the manuscript.

ADDITIONAL INFORMATION

The online version of this article (https://doi.org/10.1038/s41385-020-0293-7) contains supplementary material, which is available to authorized users.

Competing interests: The authors declare no competing interests.

Publisher's note Springer Nature remains neutral with regard to jurisdictional claims in published maps and institutional affiliations.

REFERENCES

1. Hall, C. B. et al. The burden of respiratory syncytial virus infection in young children. *N. Engl. J. Med.* **360**, 588–598 (2009).
2. Shaw, C. A. et al. The path to an RSV vaccine. *Curr. Opin. Virol.* **3**, 332–342 (2013).
3. Kim, H. W. et al. Respiratory syncytial virus disease in infants despite prior administration of antigenic inactivated vaccine. *Am. J. Epidemiol.* **89**, 422–434 (1969).
4. Castilow, E. M., Olson, M. R. & Varga, S. M. Understanding respiratory syncytial virus (RSV) vaccine-enhanced disease. *Immunol. Res.* **39**, 225–239 (2007).
5. Ruckwardt, T. J., Morabito, K. M. & Graham, B. S. Determinants of early life immune responses to RSV infection. *Curr. Opin. Virol.* **16**, 151–157 (2016).
6. Fonseca, W., Lukacs, N. W. & Ptaschinski, C. Factors affecting the immunity to respiratory syncytial virus: from epigenetics to microbiome. *Front. Immunol.* **9**, 226 (2018).
7. Cadwell, K. The virome in host health and disease. *Immunity* **42**, 805–813 (2015).
8. Duerkop, B. A. & Hooper, L.V. Resident viruses and their interactions with the immune system. *Nat. Immunol.* **14**, 654–659 (2013).
9. Virgin, H. W. The virome in mammalian physiology and disease. *Cell* **157**, 142–150 (2014).
10. Brodin, P. et al. Variation in the human immune system is largely driven by non-heritable influences. *Cell* **160**, 37–47 (2015).
11. Machiels, B. et al. A gammaherpesvirus provides protection against allergic asthma by inducing the replacement of resident alveolar macrophages with regulatory monocytes. *Nat. Immunol.* **18**, 1310–1320 (2017).
12. Dowd, J. B., Palermo, T., Brite, J., McDade, T. W. & Aiello, A. Seroprevalence of Epstein-Barr virus infection in U.S. children ages 6-19, 2003-2010. *PLoS ONE* **8**, e64921 (2013).
13. Sacco, R. E., Durbin, R. K. & Durbin, J. E. Animal models of respiratory syncytial virus infection and disease. *Curr. Opin. Virol.* **13**, 117–122 (2015).
14. Rosenberg, H. F. & Domachowske, J. B. Pneumonia virus of mice: severe respiratory infection in a natural host. *Immunol. Lett.* **118**, 6–12 (2008).
15. Anh, D. B. T., Faisca, P. & Desmecht, D. J.-M. Differential resistance/susceptibility patterns to pneumovirus infection among inbred mouse strains. *Am. J. Physiol. Lung Cell. Mol. Physiol.* **291**, L426–L435 (2006).
16. Percopo, C. M. et al. Pulmonary eosinophils and their role in immunopathologic responses to formalin-inactivated pneumonia virus of mice. *J. Immunol.* **183**, 604–612 (2009).
17. Anderson, V. E., Nguyen, Y. & Weinberg, J. B. Effects of allergic airway disease on mouse adenovirus type 1 respiratory infection. *Virology* **391**, 25–32 (2009).
18. Saito, F. et al. MHV68 latency modulates the host immune response to influenza A virus. *Inflammation* **36**, 1295–1303 (2013).
19. HAQUE, A. et al. Co-infection of malaria and gamma-herpesvirus: exacerbated lung inflammation or cross-protection depends on the stage of viral infection. *Clin. Exp. Immunol.* **138**, 396–404 (2004).

20. Wills-Karp, M., Santeliz, J. & Karp, C. L. The germless theory of allergic disease: revisiting the hygiene hypothesis. *Nat. Rev. Immunol.* **1**, 69–75 (2001).
21. Strachan, D. P. Hay fever, hygiene, and household size. *BMJ* **299**, 1259–1260 (1989).
22. Haspeslagh, E., Heyndrickx, I., Hammad, H. & Lambrecht, B. N. The hygiene hypothesis: immunological mechanisms of airway tolerance. *Curr. Opin. Immunol.* **54**, 102–108 (2018).
23. Barton, E., Mandal, P. & Speck, S. H. Pathogenesis and host control of gammaherpesviruses: lessons from the mouse. *Annu. Rev. Immunol.* **29**, 351–397 (2011).
24. Mesnil, C. et al. Lung-resident eosinophils represent a distinct regulatory eosinophil subset. *J. Clin. Investig.* **126**, 3279–3295 (2016).
25. Hegazy, A. N. et al. Interferons direct Th2 cell reprogramming to generate a stable GATA-3+T-bet+ cell subset with combined Th2 and Th1 cell functions. *Immunity* **32**, 116–128 (2010).
26. Kim, B.-S. et al. Conversion of Th2 memory cells into Foxp3 + regulatory T cells suppressing Th2-mediated allergic asthma. https://doi.org/10.1073/pnas.0911756107.
27. Dyer, K. D., Percopo, C. M., Fischer, E. R., Gabryszewski, S. J. & Rosenberg, H. F. Pneumoviruses infect eosinophils and elicit MyD88-dependent release of chemoattractant cytokines and interleukin-6. *Blood* **114**, 2649–2656 (2009).
28. Percopo, C. M. et al. Critical adverse impact of IL-6 in acute pneumovirus infection. *J. Immunol.* **202**, 871–882 (2019).
29. Essers, M. A. et al. IFNalpha activates dormant haematopoietic stem cells in vivo. *Nature* **458**, 904–908 (2009).
30. Soudja, S. M., Ruiz, A. L., Marie, J. C. & Lauvau, G. Inflammatory monocytes activate memory CD8(+) T and innate NK lymphocytes independent of cognate antigen during microbial pathogen invasion. *Immunity* **37**, 549–562 (2012).
31. Askenase, M. H. et al. Bone-Marrow-resident NK cells prime monocytes for regulatory function during Infection. *Immunity* **42**, 1130–1142 (2015).
32. Mack, M. et al. Expression and characterization of the chemokine receptors CCR2 and CCR5 in mice. *J. Immunol.* **166**, 4697–4704 (2001).
33. Jacoby, M. A., Virgin, H. W.4th, & Speck, S. H. Disruption of the M2 gene of murine gammaherpesvirus 68 alters splenic latency following intranasal, but not intraperitoneal, inoculation. *J. Virol.* **76**, 1790–1801 (2002).
34. Marshall, D. R. et al. Effector CD8+ T cells recovered from an influenza pneumonia differentiate to a state of focused gene expression. *Proc. Natl Acad. Sci. USA* **102**, 6074–6079 (2005).
35. Kohlmeier, J. E. et al. Interferons regulate cytolytic activity of memory CD8+ T cells in the lung airways during respiratory virus challenge. *Immunity* **33**, 96–105 (2010).
36. Brodin, P. & Davis, M. M. Human immune system variation. *Nat. Rev. Immunol.* **17**, 21–29 (2017).
37. Hijano, D. R. et al. Role of Type I interferon (IFN) in the respiratory syncytial virus (RSV) immune response and disease severity. *Front. Immunol.* **10**, 566 (2019).
38. Graham, B. S. Vaccine development for respiratory syncytial virus. *Curr. Opin. Virol.* **23**, 107–112 (2017).
39. Walzl, G., Tafuro, S., Moss, P., Openshaw, P. J. & Hussell, T. Influenza virus lung infection protects from respiratory syncytial virus-induced immunopathology. *J. Exp. Med.* **192**, 1317–1326 (2000).
40. Fonseca, W. et al. Lactobacillus johnsonii supplementation attenuates respiratory viral infection via metabolic reprogramming and immune cell modulation. *Mucosal Immunol.* **10**, 1569–1580 (2017).
41. Selin, L. K., Varga, S. M., Wong, I. C. & Welsh, R. M. Protective heterologous antiviral immunity and enhanced immunopathogenesis mediated by memory T cell populations. *J. Exp. Med.* **188**, 1705–1715 (1998).
42. Welsh, R. M. & Selin, L. K. No one is naive: the significance of heterologous T-cell immunity. *Nat. Rev. Immunol.* **2**, 417–426 (2002).
43. Graham, B. S., Bunton, L. A., Wright, P. F. & Karzon, D. T. Role of T lymphocyte subsets in the pathogenesis of primary infection and rechallenge with respiratory syncytial virus in mice. *J. Clin. Investig.* **88**, 1026–1033 (1991).
44. Graham, B. S., Rutigliano, J. A. & Johnson, T. R. Respiratory syncytial virus immunobiology and pathogenesis. *Virology* **297**, 1–7 (2002).
45. Schmidt, M. E. & Varga, S. M. Cytokines and CD8 T cell immunity during respiratory syncytial virus infection. *Cytokine* (2018). https://doi.org/10.1016/j.cyto.2018.07.012.
46. Welliver, T. P. et al. Severe human lower respiratory tract illness caused by respiratory syncytial virus and influenza virus is characterized by the absence of pulmonary cytotoxic lymphocyte responses. *J. Infect. Dis.* **195**, 1126–1136 (2007).
47. Openshaw, P. J. M. & Tregoning, J. S. Immune responses and disease enhancement during respiratory syncytial virus infection. *Clin. Microbiol. Rev.* **18**, 541–555 (2005).
48. Schmidt, M. E. et al. Memory CD8 T cells mediate severe immunopathology following respiratory syncytial virus infection. *PLoS Pathog.* **14**, 1–24 (2018).
49. Kim, C. K. et al. Bronchoalveolar lavage cellular composition in acute asthma and acute bronchiolitis. *J. Pediatr.* **137**, 517–522 (2000).
50. Chu, T. et al. Bystander-activated memory CD8 T cells control early pathogen load in an innate-like, NKG2D-dependent manner. *Cell Rep.* **3**, 701–708 (2013).
51. Kim, J. et al. Innate-like cytotoxic function of bystander-activated CD8 + T cells is associated with liver injury in acute hepatitis A. *Immunity* **48**, 161–173 (2018). e5.
52. Schenkel, J. M. et al. Resident memory CD8 t cells trigger protective innate and adaptive immune responses. *Science* **346**, 98–101 (2014).
53. Nakamura, Y. et al. Helper function of memory CD8+ T cells: heterologous CD8 + T cells support the induction of therapeutic cancer immunity. *Cancer Res.* **67**, 10012–10018 (2007).
54. Molloy, M. J., Zhang, W. & Usherwood, E. J. Suppressive CD8 + T cells arise in the absence of CD4 help and compromise control of persistent virus. *J. Immunol.* **186**, 6218–6226 (2011).
55. Yao, Y. et al. Induction of autonomous memory alveolar macrophages requires T cell help and is critical to article induction of autonomous memory alveolar macrophages requires T cell help. *Cell* 1–17 (2018). https://doi.org/10.1016/j.cell.2018.09.042.
56. Dyer, K. D. et al. Priming of the respiratory tract with immunobiotic *Lactobacillus plantarum* limits infection of alveolar macrophages with recombinant pneumonia virus of mice (rK2-PVM). *J. Virol.* **90**, 979–991 (2016).
57. Rigaux, P., Killoran, K. E., Qiu, Z. & Rosenberg, H. F. Depletion of alveolar macrophages prolongs survival in response to acute pneumovirus infection. *Virology* **422**, 338–345 (2012).
58. Latif, M. B. et al. Deletion of murid herpesvirus 4 ORF63 affects the trafficking of incoming capsids toward the nucleus. *J. Virol.* **90**, 2455–2472 (2016).